NADPH oxidase-derived H_2O_2 subverts pathogen signaling by oxidative phosphotyrosine conversion to PB-DOPA

Luis A. Alvarez[a], Lidija Kovačič[b,1], Javier Rodríguez[c,2], Jan-Hendrik Gosemann[a,3], Malgorzata Kubica[b], Gratiela G. Pircalabioru[b,4], Florian Friedmacher[a], Ada Cean[d], Alina Ghişe[d], Mihai B. Sărăndan[d], Prem Puri[a], Simon Daff[e], Erika Plettner[f], Alex von Kriegsheim[c,2], Billy Bourke[a,b,5,6], and Ulla G. Knaus[a,b,5,6]

[a]National Children's Research Center, Our Lady's Children's Hospital Crumlin, Dublin 12, Ireland; [b]Conway Institute, School of Medicine, University College Dublin, Dublin 4, Ireland; [c]Systems Biology Ireland, University College Dublin, Dublin 4, Ireland; [d]Faculty of Veterinary Medicine, Banat University of Agricultural Sciences and Veterinary Medicine "King Michael I of Romania", 300645 Timisoara, Romania; [e]School of Chemistry, University of Edinburgh, Edinburgh EH9 3F, United Kingdom; and [f]Department of Chemistry, Simon Fraser University, Burnaby, BC V5A 1S6, Canada

Edited by Judith P. Klinman, University of California, Berkeley, CA, and approved July 19, 2016 (received for review April 4, 2016)

Strengthening the host immune system to fully exploit its potential as antimicrobial defense is vital in countering antibiotic resistance. Chemical compounds released during bidirectional host–pathogen cross-talk, which follows a sensing-response paradigm, can serve as protective mediators. A potent, diffusible messenger is hydrogen peroxide (H_2O_2), but its consequences on extracellular pathogens are unknown. Here we show that H_2O_2, released by the host on pathogen contact, subverts the tyrosine signaling network of a number of bacteria accustomed to low-oxygen environments. This defense mechanism uses heme-containing bacterial enzymes with peroxidase-like activity to facilitate phosphotyrosine (p-Tyr) oxidation. An intrabacterial reaction converts p-Tyr to protein-bound dopa (PB-DOPA) via a tyrosinyl radical intermediate, thereby altering antioxidant defense and inactivating enzymes involved in polysaccharide biosynthesis and metabolism. Disruption of bacterial signaling by DOPA modification reveals an infection containment strategy that weakens bacterial fitness and could be a blueprint for antivirulence approaches.

mucosal immunity | NADPH oxidase | bacterial tyrosine phosphorylation | DOPA | reactive oxygen species (ROS)

Communication between the host and pathogens at the mucosal interface is governed by the chemical environment. Host-derived signals can be subverted by pathogens to enhance virulence gene expression and pathogen expansion (1), but in most circumstances the immune system prevails by coordinating defense mechanisms, thereby restricting colonization and disease. Within complex mucosal environments, pathogen virulence can be modulated in a niche-specific manner (2), which is now recognized as an important strategy that helps combating antibacterial resistance. The most promising approach to target bacterial virulence factors is through the use of compounds that affect multiple prokaryotic targets at once.

As a relatively stable, diffusible mediator host-derived hydrogen peroxide (H_2O_2) can modify more distant targets. H_2O_2 can penetrate bacterial membranes inducing transcriptional stress responses (3), but may also alter other cellular processes via oxidation. High concentrations of reactive oxygen species (ROS) and derivatives (HOCl) can induce irreversible amino acid oxidations or chlorinations, leading to loss of function by misfolding or degradation and to bacterial killing. Lower ROS levels, in particular H_2O_2, primarily result in oxidative modifications that are dynamic and reversible, such as thiol oxidation and disulfide bond formation in enzymes, iron-sulfur clusters, or transcriptional regulators containing redox-sensitive cysteine residues. The redox sensitivity of mammalian tyrosine kinase pathways is mainly a result of transient inactivation of protein tyrosine phosphatases or by oxidative protein kinase activation (e.g., SRC, ASK1) (4). Intestinal pathogens traversing through the mucus before attaching to or invading the epithelium can activate epithelial NADPH oxidases (NOX1, DUOX2) before recruitment of neutrophils occurs. Neutrophils engulfing bacteria produce and release large quantities of $O_2^{\bullet-}$ via NOX2 into the phagosome, which enables bacterial killing by the concerted action of HOCl, proteases, and antibacterial peptides (5). Intestinal epithelial cells (IEC) release low levels of H_2O_2 into the lumen, but the achievable concentrations are in the nano/micromolar range and inadequate for bactericidal activity. We hypothesized that, when maintained over time, IEC-derived H_2O_2 may overcome antioxidant defenses of pathogens and may alter redox-regulated processes in bacteria.

Bearing in mind how H_2O_2 acts on mammalian signaling circuits, the prime target for redox regulation in prokaryotes are tyrosine kinase pathways. Tyrosine phosphorylation coordinates a variety of key processes in bacteria, including biofilm and capsule formation, heat-shock response, DNA replication, transcription, metabolic processes, antibiotic resistance, virulence, and

Significance

Mucosal barrier tissues participate in immune defense in infections, but NADPH oxidases expressed in these epithelia are much less efficient in their oxidant output than the phagocyte oxidase. The importance of releasing low hydrogen peroxide (H_2O_2) concentrations as a host defense mechanism against pathogens remains unclear. Here, we demonstrate that nano to submicromolar H_2O_2 disrupts the tyrosine phosphorylation network in several pathogens by an oxidative dephosphorylation process; this is accomplished by irreversible chemical modification of key phosphotyrosine residues, which in turn changes protein activity without affecting bacterial viability. This process is a host-initiated antivirulence strategy, reducing the fitness of pathogens in the extracellular space.

Author contributions: L.A.A., E.P., A.v.K., B.B., and U.G.K. designed research; L.A.A., L.K., J.R., J.-H.G., M.K., G.G.P., F.F., A.C., A.G., and M.B.S. performed research; P.P. and S.D. contributed new reagents/analytic tools; L.A.A., L.K., J.R., A.v.K., B.B., and U.G.K. analyzed data; and L.A.A., E.P., B.B., and U.G.K. wrote the paper.

The authors declare no conflict of interest.

This article is a PNAS Direct Submission.

[1]Present address: Novartis Ireland Ltd, Dublin 2, Ireland.

[2]Present address: Edinburgh Cancer Research Center, University of Edinburgh, Edinburgh EH4 2XR, United Kingdom.

[3]Present address: Department of Pediatric Surgery, University of Leipzig, 04103 Leipzig, Germany.

[4]Present address: The Research Institute of the University of Bucharest, 050107 Bucharest, Romania.

[5]B.B. and U.G.K. contributed equally to this work.

[6]To whom correspondence may be addressed. Email: billy.bourke@ucd.ie or ulla.knaus@ucd.ie.

This article contains supporting information online at www.pnas.org/lookup/suppl/doi:10.1073/pnas.1605443113/-/DCSupplemental.

interspecies communication (6). Bacterial tyrosine (BY) kinases contain ATP-binding Walker motifs and a C-terminal tyrosine cluster, and exhibit no sequence or structural homology to eukaryotic kinases (7). These BY-kinases cooperate with phosphatases, various association partners, and Hanks type serine/threonine kinases in interaction networks, but mechanistic details of their regulation and often even the identity of the kinases remain poorly understood. Nevertheless, interfering with BY-kinase signaling should be beneficial because decreased virulence has been connected to interference with BY-kinase pathways (8, 9). Here we show that H_2O_2-mediated disruption of bacterial tyrosine signaling is a common feature in intestinal and even pulmonary pathogens, requiring low H_2O_2 concentrations in physiological conditions and a combination of host and bacterial features present in oxygen-restricted environments during infections. In contrast to increased phosphotyrosine (p-Tyr) signaling by phosphatase inhibition via thiol oxidation in mammalian systems, H_2O_2 triggered iron-associated conversion of p-Tyr to DOPA on bacterial proteins, leading to disruption of p-Tyr signaling. Proteomics data reveal that this interference with p-Tyr signaling occurs frequently in prokaryotic and eukaryotic organisms.

Results

H_2O_2 Disrupts Phosphotyrosine Signaling of Pathogens. The pathogens *Listeria monocytogenes*, *Salmonella enterica* serovar Typhimurium and *Klebsiella pneumoniae* were chosen as representative enteric bacteria with diverse cell wall structures, motility, and antioxidant defense gene expression to determine if host epithelial H_2O_2 production accompanies intestinal infection as a general defense mechanism. All of these bacteria induced H_2O_2 release when incubated with IECs (HCT-8 cells) (Fig. 1*A*), an effect suppressed by the cell-permeable pan-oxidase inhibitor diphenyleneiodonium chloride (DPI) and catalase. Previously, we connected H_2O_2 generation upon pathogen contact in this cell type directly to NOX1, the only NADPH oxidase expressed (8). Bacterial infection triggered translocation of the NOX-p22^{phox} complex to the plasma membrane (Fig. S1*A*; visualized as p22^{phox}), inducing continuous release of low H_2O_2 concentrations (20 nmol H_2O_2/h per milligram of protein). A similar H_2O_2 concentration is achieved on top of a Boyden chamber filter with Cos cells expressing constitutively active NOX4 seeded on the bottom (15 nmol H_2O_2/h per milligram of protein) (8) (Fig. 1*A*). In human colon biopsies, a physiologically relevant model expressing NOX1, *L. monocytogenes* infection caused up-regulation and membrane recruitment of the NOX-p22^{phox} complex concurrently with H_2O_2 generation (Fig. 1*B* and Fig. S1*B*). ROS generation was also detected in vivo using a ligated rabbit ileal loop infection model. Injection of *L. monocytogenes* or *Campylobacter jejuni* led to severe tissue injury in rabbits, preceded by recruitment of the NOX dimerization partner p22^{phox} to the apical crypt surface and oxidative modification of epithelia by carbonylation (Fig. 1*C* and Fig. S1 *C–E*). These data indicate that gut epithelial H_2O_2 generation by NADPH oxidase is commonly observed in infection.

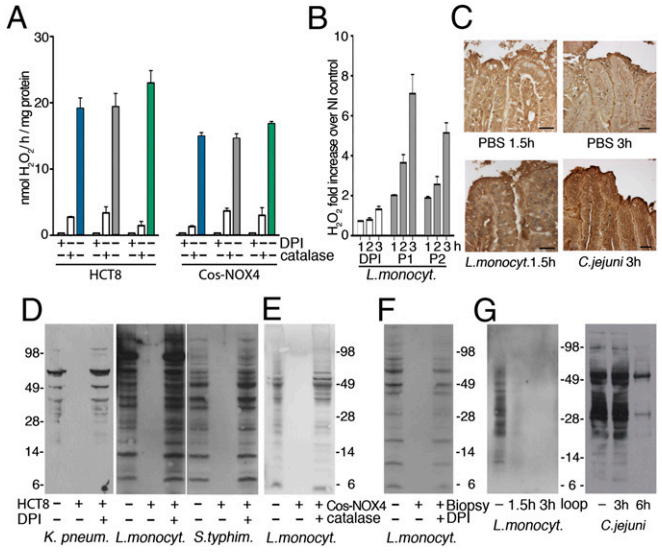

Fig. 1. Mucosal H_2O_2 leads to tyrosine dephosphorylation in intestinal bacteria. (*A*) H_2O_2 release by IECs (HCT-8) following exposure to enteric bacteria (±DPI or catalase addition) and by Cos-NOX4 cells separated from bacteria by a filter (*K. pneumoniae*, blue; *L. monocytogenes*, gray; *S. typhimurium*, green). (*B*) H_2O_2 release by colonic biopsies after infection with *L. monocytogenes* (patients P1, P2). Control is DPI preincubation of biopsies. (*C*) Carbonylation of rabbit ileal loop tissues after injection with PBS, *L. monocytogenes* (1.5 h) or *C. jejuni* (3 h). (Scale bars, 25 μm.) (*D* and *E*) Anti–p-Tyr immunoblots of lysates derived from extracellular bacteria exposed to IEC (*D*) or Cos-NOX4 (*E*) for 3 h (see *A*). (*F*) Anti–p-Tyr immunoblot of extracellular *L. monocytogenes* after exposure to biopsies (see *B*) (3 h). Starting culture is used for comparison. (*G*) Anti–p-Tyr immunoblot of *L. monocytogenes* or *C. jejuni* recovered from the ileal loop lumen.

The majority of bacteria remain extracellular in the mucus layer or gut lumen at any particular time point of infection, either because only a certain fraction will invade epithelial cells (e.g., *Listeria*) or because particular pathogens attach to but do not invade IECs (e.g., *Klebsiella*). Released H_2O_2 is taken up by bacteria and induces a transcriptional stress response, but we speculated that H_2O_2 may also alter tyrosine kinase pathways. Immunoblot analysis of extracellular bacteria recovered from media of infected IECs, from the top of the filter of Cos-NOX4 cells or from biopsy media, revealed not increased but significantly decreased bacterial p-Tyr content when H_2O_2 was present (Fig. 1 *D–F*). Bacterial viability or overall bacterial protein content were not altered (Figs. S1 *F–I* and S2*B*).Tyrosine phosphorylation of Wzc, the main BY-kinase expressed in *K. pneumoniae*, *Escherichia coli*, and *Acinetobacter* (7), was substantially lower, but Wzc expression was not altered (Fig. S2*A*). These observations were further confirmed by analyzing bacteria recovered from the rabbit ileal lumen after infection. Overall tyrosine phosphorylation was significantly diminished in extracellular bacteria, whereas protein content was comparable to the starting bacterial culture (Fig. 1*G* and Fig. 1*J*).

Mancini and Imlay (10) reported that a bacterial culture in iron-rich media decomposed 0.5 mM H_2O_2 in less than 2 h without affecting bacterial growth substantially, and an intracellular H_2O_2 sensor indicated an up to 500-fold gradient between outside and inside H_2O_2 concentrations in *E. coli* (11). In line with these observations, addition of 0.7 mM H_2O_2 to bacterial cultures mimicked tissue-based observations without reducing bacterial viability (Fig. S2*B*), whereas heat treatment did not alter the p-Tyr profile (Fig. S2 *C* and *D*). Bacterial tyrosine phosphorylation has been connected to pathogenicity (8, 9) and to type 3 secretion system regulation in enterohemorrhagic *E. coli* (12). If a similar link exists between p-Tyr signaling and *L. monocytogenes* virulence, it should be disrupted by H_2O_2. In accord, adhesion to IECs, which is a prerequisite for *Listeria* invasion, decreased significantly after pre-exposure of *L. monocytogenes* to H_2O_2, resulting in lower internalization of the bacterium (Fig. S2*E*). Oxidative tyrosine dephosphorylation may occur also at other mucosal surfaces, in particular in the lung where ROS generated by alveolar macrophages and lung epithelial cells provide host defense. We established a fetal rat lung model that permitted intraorgan incubation with bacteria and subsequent recovery of bacteria and bronchoalveolar fluid. Intratracheal injection of *Streptococcus pneumoniae* caused two- to threefold increased H_2O_2 levels above the DPI baseline with concomitant decrease of the p-Tyr content in bacteria recovered from the bronchoalveolar fluid pellet (Fig. S3 *A* and *B*). The developmental regulation of DUOX expression and the short period of pathogen exposure favored macrophages as an H_2O_2 source in this model. Coculture of *S. pneumoniae* with rat alveolar macrophages prompted increased cell adhesion and protrusions that were accompanied by NOX2 NADPH oxidase up-regulation, translocation of NOX2 to the plasma membrane, and $O_2^{\bullet-}$/H_2O_2

MICROBIOLOGY

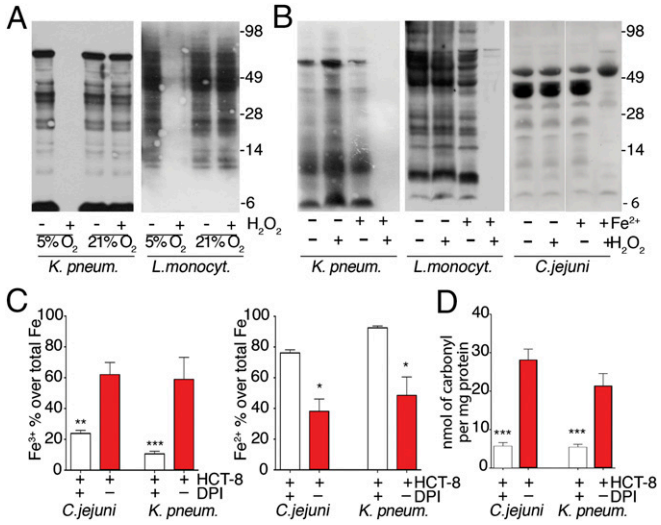

Fig. 2. Oxygen and iron availability affect oxidative dephosphorylation of tyrosines. (*A* and *B*) Anti–p-Tyr immunoblots of bacteria cultured in 5% or 21% O_2 (*A*) or in low- or high-iron conditions at 5% O_2 (*B*) before 0.7 mM H_2O_2 addition (3 h). (*C*) Quantification of Fe^{3+} vs. Fe^{2+} in indicated bacteria cocultured with HCT-8 cells (±DPI pretreatment). (*D*) Quantification of carbonyl formation in *C. jejuni* or *K. pneumoniae* protein extracts after HCT-8 coculture. Error bars represent SEM and asterisks indicate significance (***$P \leq 0.001$, **$P \leq 0.01$, and *$P \leq 0.05$).

production, which was inhibited by DPI (Fig. S3 *C* and *D*). *S. pneumoniae* itself was not affected by DPI and did not generate H_2O_2 in the low-oxygen conditions used throughout (Fig. S3*E*). Decreased p-Tyr content was detected in extracellular *S. pneumoniae* collected from macrophage coculture media, similar to our observations in infected rat lungs (Fig. S3*F*). Adding H_2O_2 as single bolus to growth medium induced *S. pneumoniae* tyrosine dephosphorylation without altering bacterial viability (Fig. S3*G*). Polysaccharide biosynthesis is to date the only well-characterized process regulated by bacterial tyrosine phosphorylation. Pre-exposure of *S. pneumoniae* to H_2O_2 diminished biofilm formation (Fig. S3 *H* and *I*), thus strengthening the connection between H_2O_2, tyrosine dephosphorylation, and pathogenic traits. These results indicate that host H_2O_2 production is coupled to diminished p-Tyr content in extracellular pathogens, leading to decreased pathogenicity by disrupting intrabacterial signaling.

The Chemical Microenvironment and Hemoproteins Affect Oxidative Tyrosine Dephosphorylation in Bacteria. The change in bacterial p-Tyr content by oxidation suggested a distinct mechanism for phosphate group removal, as thiol-based inactivation of phosphatases would cause increased tyrosine phosphorylation. Furthermore, deletion of PTP1B, the only known phosphatase in *C. jejuni*, did not alter p-Tyr–dependent capsule biosynthesis. We explored the environmental conditions required for the suppression of bacterial p-Tyr by H_2O_2. Intestinal pathogens are typically facultative anaerobes, thriving in the low oxygen levels present in the gut (13), but many bacteria tolerate atmospheric oxygen levels. Environmental adaptation prompts usually global transcriptional responses (14), but these external stress signals may also remodel the bacterial signaling conduit. Comparison of bacteria propagated in low oxygen (5% O_2) versus ambient oxygen (21% O_2) before exposure to H_2O_2 indicated a striking difference. *K. pneumoniae* and *L. monocytogenes* grown in 21% O_2 before addition of H_2O_2 retained their original p-Tyr profile, whereas cultures grown in 5% O_2 lost the p-Tyr signal (Fig. 2*A*).

We questioned whether changes in iron availability could affect the p-Tyr network, as oxidative stress in bacteria can induce iron regulators (e.g., Fur, Dps) and inactivate iron-sulfur dehydratases (3). Bacterial cultures initially grown in iron-deficient media at 5% O_2 were analyzed after addition of ferrous sulfate and H_2O_2. The p-Tyr content was only diminished by H_2O_2 when extracellular iron was provided (Fig. 2*B*). In coculture conditions where iron is supplied by HCT-8 cells and the culture media, the Fe^{2+} versus Fe^{3+} ratio in the total pool of bacterial intracellular iron was dependent on IEC-mediated H_2O_2 generation (Fig. 2*C*), suggesting that the bacterial intracellular pool of free ferrous iron was oxidized to ferric iron. Carbonylation, a marker for site-specific, metal-catalyzed protein modification by hydroxyl radicals, was increased in bacteria exposed to HCT-8–generated H_2O_2 (Fig. 2*D*). This finding suggests that oxidative tyrosine dephosphorylation in bacteria is taking place in conditions that are present in the intestine during infections.

Cytochrome P450 or Peroxidase Activity Is Required for Oxidative Dephosphorylation. Many pathogens, including certain *Pseudomonas*, *Mycobacterium*, or *Acinetobacter* strains, contain cytochrome P450 monooxygenases that catalyze hydroxylation reactions via molecular oxygen reduction or by using the peroxide-shunt pathway, contributing to virulence and persistence in the host (15). Expression of an outer membrane/periplasmic cytochrome P450 (Cj1411, CjP450) in *C. jejuni* increased after H_2O_2 exposure and deletion of CjP450 decreased capsular polysaccharide production (16), raising the possibility that CjP450 participates in p-Tyr signaling. Deletion of CjP450 or mutation of a cysteine (C.j. *ΔP450:P450C399F*) in the heme-iron ligand signature motif of CjP450 that leads to perturbation of the heme pocket and loss of catalytic activity in P450 enzymes,

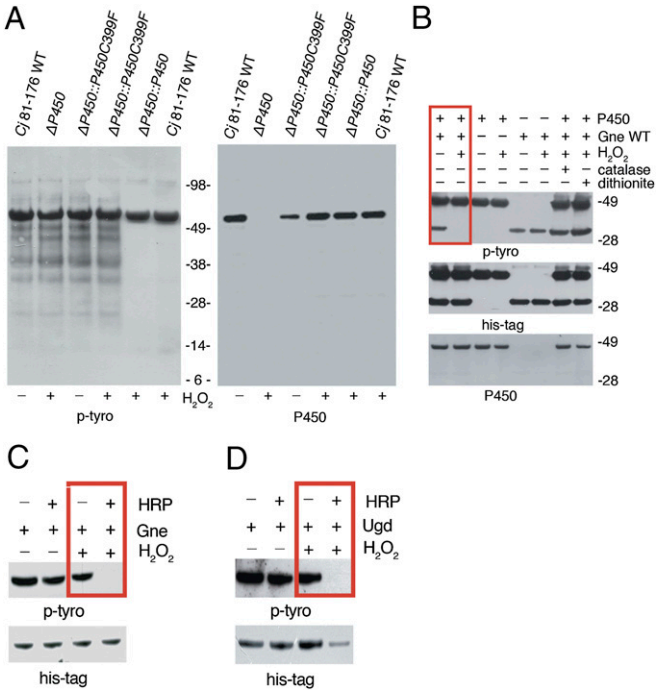

Fig. 3. Cytochrome P450 or peroxidases are required for oxidative phosphate removal. (*A*) Anti–p-Tyr immunoblot of *C. jejuni* strains with or without exposure to H_2O_2. *C. jejuni* 81-176 (WT) was compared with *C. jejuni Δcjj81176_1410* (*ΔP450*), to the P450 reconstituted strain (*ΔP450::P450*), or to *C. jejuni ΔP450* reconstituted with P450 active site cysteine mutant (*ΔP450::P450 C399F*). Blots were reprobed with anti-P450 antibody. (*B*) Tyrosine dephosphorylation of *C. jejuni* Gne by *C. jejuni* cytochrome P450 in the presence or absence of 1 mM H_2O_2. Catalase and dithionite served as controls for H_2O_2 and P450 activity, respectively. Anti–p-Tyr, anti-His tag, and anti-P450 immunoblots are shown. (*C*) Tyrosine dephosphorylation of Gne by HRP in the presence or absence of 1 mM H_2O_2. (*D*) Tyrosine dephosphorylation of *E. coli* Ugd by HRP in the presence or absence of 1 mM H_2O_2.

rendered the *C. jejuni* p-Tyr network insensitive to H_2O_2 (Fig. 3*A*). To verify direct participation of CjP450 in oxidative tyrosine dephosphorylation, both CjP450 and Gne, a UDP-GlcNAc/Glc 4-epimerase phosphorylated on the active site Tyr^{146}, were expressed and purified from *E. coli* (Fig. S4*A*) (16). Dephosphorylation of Gne was dependent on addition of H_2O_2 and CjP450, and not observed in the presence of catalase and sodium dithionite, respectively (Fig. 3*B*). When H_2O_2 is available, cytochrome P450s can exhibit peroxidase-like activity (15, 17). We asked if other hemoproteins, such as HRP, could catalyze this reaction in a similar fashion. Replacing CjP450 with HRP during exposure of Gne to H_2O_2 removed p-Tyr equally efficiently (Fig. 3*C*).

To date, Gne is the only characterized BY-kinase substrate in *C. jejuni*, impeding analysis of other p-Tyr–containing proteins in this bacterium. Using 2D gel electrophoresis of *C. jejuni* outer membrane fractions followed by p-Tyr detection and MS, we identified CetB (Cj1189c), a protein involved in energy taxis and motility (18), as a tyrosine kinase substrate (Fig. S4*B*). CetB, cloned from *C. jejuni* 81-176, was expressed and purified using *E. coli* (Fig. S4*C*). As with Gne, CetB was also tyrosine phosphorylated by *E. coli* BY-kinases, reflecting the relaxed substrate specificity of bacterial tyrosine kinases (19). CetB was dephosphorylated on tyrosine only when H_2O_2 and cytochrome P450 were present (Fig. S4*D*). Many bacteria, including *E. coli*, do not express cytochrome P450 enzymes, but they contain heme peroxidases. A comparable decrease in p-Tyr was observed when purified recombinant UDP-glucose dehydrogenase (Ugd), a BY-kinase substrate expressed in *K. pneumoniae* and other bacteria, was treated with HRP in the presence of H_2O_2 (Fig. 3*D* and Fig. S4*E*). Ugd, which catalyzes the synthesis of UDP-glucuronic acid, is activated by phosphorylation of Tyr^{71}, and regulates capsule biosynthesis and colanic acid production (20). This result emphasizes the connection between H_2O_2-induced tyrosine dephosphorylation and attenuation of pathogenicity determinants.

H_2O_2-Induced Conversion of Phosphotyrosine to Protein-Bound DOPA. To understand how tyrosine dephosphorylation occurs, we sought to identify the final product of this reaction by MS analysis of peptides derived from recombinant Gne or Ugd after exposure to H_2O_2 and HRP. In particular, both bacterial proteins contain phosphorylated key tyrosyl residues in their active site (Gne Tyr^{146}) or as cofactor affinity enhancer (Ugd Tyr^{71}) (20, 21), which are important for polysaccharide biosynthesis. Peptides containing these tyrosines were found to be oxidized by exogenous H_2O_2, leading to $^{\bullet}$OH-induced DOPA formation (Fig. 4 *A* and *B* and Fig. S5). To ensure that the loss of tyrosine phosphorylation did not arise from variations in turnover of the limited pool of p-Tyr proteins, we determined concomitant loss of the p-Tyr signal and DOPA addition by performing analogous experiments using CjP450 (or HRP) together with a synthetic phosphopeptide (100% p-Tyr), comprising the sequence surrounding Gne Tyr^{146} in the presence of H_2O_2. The MS/MS spectra confirmed substantial loss of the phosphate group on tyrosine and matching DOPA modification, resulting in a net mass change of 63 Da on modified tyrosines (Fig. 4 *C* and *D* and Fig. S6 *A*–*D*). Quantification revealed that the increase in DOPA signal in the peptide was accompanied by a decrease in the phosphorylated peptide (Fig. 4*E*).

A number of potential chemical mechanisms can be invoked to explain the conversion of p-Tyr to DOPA (Fig. S7). The source for hydroxylation could be water (reaction 1) or H_2O_2 (reactions 2 and 3). Because $H_2{}^{18}O_2$ labeled DOPA (Fig. 4 *C* and *D* and Fig. S6*D*), we ruled out reaction 1. Reaction 2 would proceed via a 2-hydroxy-3,5-cyclohexadienone intermediate, whereas reaction 3 would predict generation of a tyrosinyl radical intermediate (Fig. S7, red box) (22, 23). The addition of free tyrosine to the oxidation reaction will discriminate between these two possibilities, because only a tyrosinyl radical intermediate will permit dityrosine formation. Nano LC-MS/MS analysis of the synthetic phosphopeptide, or of Gne and Ugd treated with H_2O_2 in the presence of L-tyrosine and CjP450 (or HRP), indicated dityrosine formation at active-site tyrosines with a net mass change of 100 Da (Fig. 4 *C*, *D*, *F*. and *G*

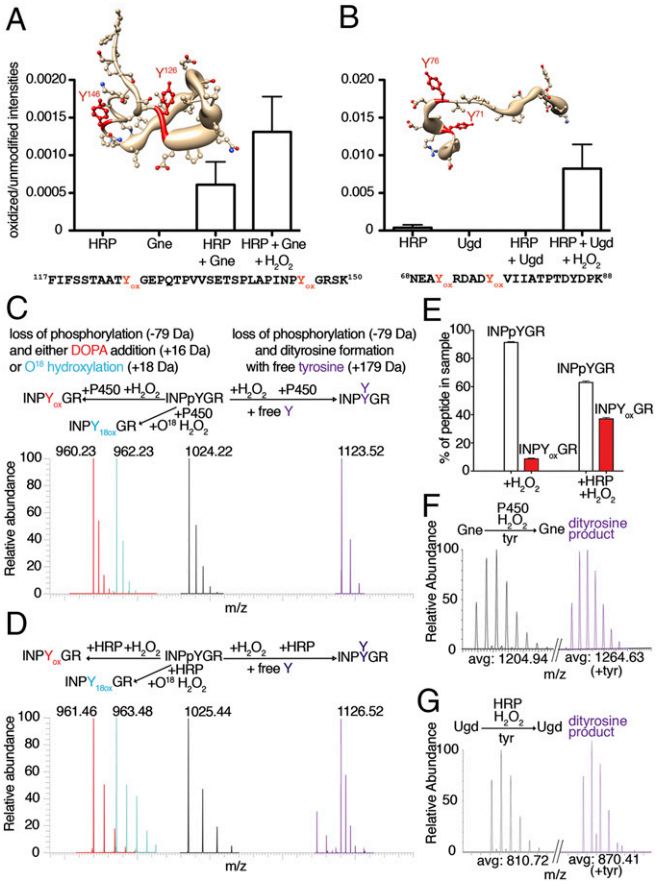

Fig. 4. DOPA modification displaces phosphate via tyrosinyl radical formation. (*A* and *B*) Oxidized over unmodified peptide intensities of (*A*) the Gne peptide (amino acids 117–150) containing Tyr^{146} and of (*B*) the Ugd peptide (amino acids 68–88) containing Tyr^{71} in the MS spectra. Y_{ox} indicates DOPA-modified tyrosine. Localization of oxidized tyrosine residues is shown in worm-style with width proportional to residue accessibility and in the peptide sequence. (*C* and *D*) MS spectra of a synthetic phosphotyrosine peptide (biotin-INPpYGR) after treatment with 1 mM H_2O_2 and either (*C*) CjP450 or (*D*) HRP. The starting phosphorylated peptide is in black, DOPA in red, dityrosine formation in purple, and ^{18}O oxidation in cyan. The reactions leading to each modification are indicated. (*E*) Quantification of pY vs. Y_{ox} in the synthetic INPpYGR peptide upon exposure to 1 mM $H_2O_2 \pm$ HRP using MS/MS. (*F* and *G*) Isotopic peak MS spectra indicating dityrosine formation (purple) for tryptic peptides derived from Gne (*F*) or Ugd (*G*) following treatment as indicated.

and Fig. S6 *C*, *E*, and *F*). These results support reaction 3 as the mechanism leading to oxidative phosphate removal and DOPA addition on tyrosine. Analysis of the solvent accessibility surface area of modified tyrosines did not provide a clear link between surface exposure, tyrosinyl radical formation, and subsequent DOPA modification (Fig. S8), suggesting that the microenvironment surrounding certain tyrosines leads to specific, nonrandom oxidation events.

***K. pneumoniae* DOPA Proteomics and Computational Chemistry Approach.** To assess bacterial protein-bound (PB) DOPA modifications globally, *K. pneumoniae* grown at 5% O_2 was exposed to a bolus of H_2O_2 or, separated by a filter, to 15–20 nmol H_2O_2/h per milligram of protein continuously released by Cos-NOX4 cells, mimicking a rate of H_2O_2 release similar to stimulated IECs (24). Without using any enrichment strategy, MS/MS analysis revealed up-regulation of the ROS scavengers superoxide dismutase (SOD, UniProtKB-M7QF58, twofold) and alkyl hydroperoxide reductase [AhpC 1.3-fold, AhpD 180-fold (by H_2O_2), AhpF twofold (by NOX4)], but not catalase (KatG). The relative abundance of PB-DOPA after treatment was increased (25–35%)

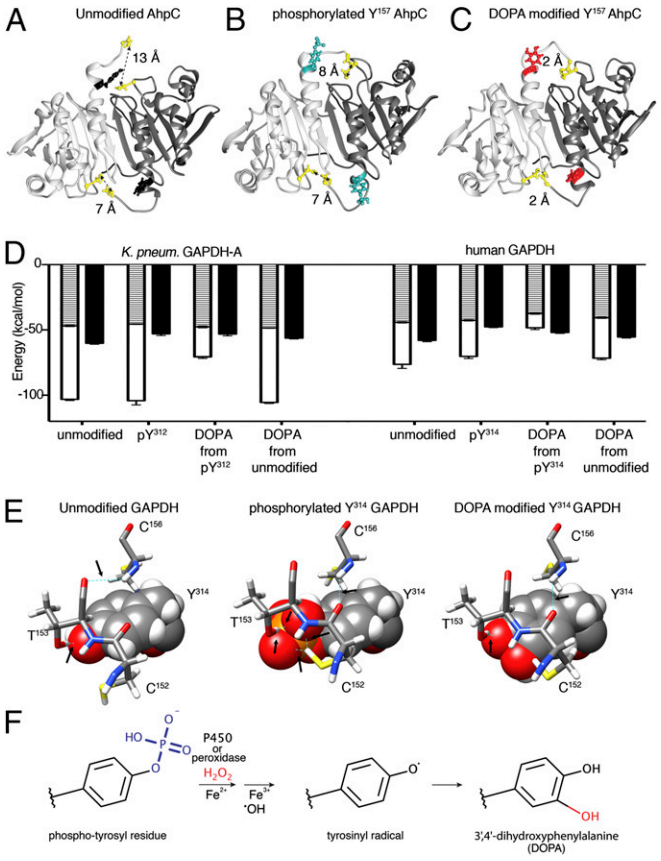

Fig. 5. DOPA modification on oxidative stress-associated *K. pneumoniae* proteins. (*A–C*) AhpC 3D model depicting Tyr^{157} in relation to Cys^{47} and Cys^{166} in unmodified (*A*), p-Tyr^{157} (*B*), and DOPA-Tyr^{157} (*C*) conformation. Cys–Cys distances indicated in Angströms. (*D*) Binding energy for NAD^+ to GAPDH (*K. pneumoniae* Tyr^{312}, human Tyr^{314}) in unmodified, phosphorylated, p-Tyr to DOPA, or unmodified to DOPA form. Van der Waals energy (hatched), electrostatic energy (white), and desolvation energy (black). (*E*) Comparison of unmodified, p-Tyr^{314}, and DOPA-Tyr^{314} human GAPDH. Tyr^{314} is shown space filling, side chains are sticks, hydrogen bonds are dashed lines in cyan, indicated with arrows. (*F*) Schematic representation of the key reactions leading to oxidative dephosphorylation of bacterial tyrosyl residues and conversion to DOPA.

over untreated conditions or when exposed to NOX4-deficient Cos-22^{phox} cells. Analysis of DOPA sites (Table S1) revealed that AhpC itself, a thiol-based peroxidase and the primary scavenger of low H_2O_2 concentrations in *E. coli* (25), was modified on Tyr^{157}, a residue previously identified as an AhpC phosphorylation site in *K. pneumoniae* and *E. coli* (9, 12). Tyr^{157} is located in the vicinity of the resolving Cys^{166} that reacts with Cys^{47} (26). We used molecular dynamics simulation of AhpC in different states to analyze disulfide bond connectivity, which revealed that the backbone regions move considerably closer together in the DOPA-modified AhpC dimer (Fig. 5 *A–C*), which may affect turnover. Thus, H_2O_2 cannot only alter tyrosines in the catalytic center of enzymes involved in metabolic and virulence-associated pathways, but also hydroxylates AhpC, the initial antioxidant defense enzyme.

Proteomics data compiled in Table S1 indicate that DOPA addition on particular tyrosine residues, identified by us in *K. pneumoniae* or reported in *E. coli* K12 grown at 21% oxygen (27), match p-Tyr modifications (9, 12). A frequently modified enzyme is GAPDH-A (gapA), which is susceptible to DOPA modification on Tyr^{312}, a residue identified also as a phosphorylation site in *E. coli* (12). GAPDH, a glycolytic enzyme and H_2O_2 sensor with peroxidatic activity, contributes to colonization and invasion (28). Tyr^{312} in *K. pneumoniae* GAPDH (Tyr^{314} in human GAPDH) represents in unmodified form a critical residue in a proton-shuttle mechanism essential for the H_2O_2 sensitivity of the enzyme (29). Molecular dynamics simulations indicated that NAD^+ binding to phosphorylated Tyr^{312} lowered the desolvation energy (~10%), whereas subsequent DOPA modification decreased the electrostatic energy by ~40% and NAD^+ binding by 50% (Fig. 5*D*). The situation for human GAPDH is similar, although the NADPH/$NADP^+$ ratio for *K. pneumoniae* GAPDH would be higher. The direct conversion from unmodified Tyr^{312} to DOPA-Tyr^{312}, a process unlikely to occur in physiological conditions, would cause less structural change than a DOPA conversion from a phosphorylated residue (Fig. 5*D*). In contrast to the increased resistance of a human GAPDH Y314F mutant to oxidative inactivation (29), conversion of p-Tyr^{314} to DOPA will be comparable to exposure of wild-type GAPDH to 200 μM H_2O_2 (29) and will not alter adaptation to oxidative stress. A subset of p-Tyr^{314} modified GAPDH might be present at any given time in mammalian tissues (30). Phosphorylated GAPDH will not require the proton relay for H_2O_2 sensitivity because the space for H_2O_2 interaction with Cys^{152} will be occupied by the phosphate group in p-Tyr^{314} and the creation of two hydrogen bonds between Cys^{152} and p-Tyr^{314} (Fig. 5*E*). Oxidative dephosphorylation and DOPA addition on Tyr^{314} will then alter NAD^+ affinity. These examples demonstrate that oxidative dephosphorylation and subsequent DOPA addition act as regulator of enzyme function, and that the outcome will differ depending on the structural and functional context. Improved techniques for detecting and stabilizing tyrosine modifications will permit discovering many more candidates for p-Tyr conversion, particularly in oxidative stress conditions.

Discussion

Phosphorylation-driven signaling networks are crucial for maintaining functional responses in all organisms. Similarly conserved is the release of diffusible mediators, in particular H_2O_2, for protection and adaptation. In mammalian systems thiol oxidation is a potent pathway modifier, often accelerating or causing disease when deregulated. In bacteria exposure to H_2O_2 concentrations in the nano to submicromolar range has been associated with oxidation of reactive cysteinyl residues and $[4Fe\text{-}4S]^{2+}$ clusters. Damaging irreversible modifications, such as methionine oxidation and 3-chlorotyrosine formation, were connected to the myeloperoxidase–H_2O_2–chloride axis and bacterial killing in the phagosome of neutrophils (5). Using a range of conditions, including host–pathogen interaction models, constant exposure of bacteria to nanomolar H_2O_2 that mimics host epithelial H_2O_2 release during infection, or to a single bolus of H_2O_2, we report here disruption of p-Tyr signaling by oxidative p-Tyr conversion to DOPA (Fig. 5*F*).

Tyrosines in the vicinity of lysines, in particular in YXX(XX)K or KXXX(X)Y motifs, seem prone to hydroxylation or chlorination (27, 31), and are also preferred phosphorylation sites in *E. coli* proteins (12). These motifs are present in the DOPA-modified bacterial proteins Gne, Ugd, AhpC, and GAPDH-A featured in this study. The nearby positive charge may favor the deprotonated form of tyrosine, facilitating phosphorylation and oxidative electron transfer. The presence of DOPA on proteins involved in ROS conversion [AhpC, SOD (27)] or in redox-sensitive processes (GAPDH-A), and the predicted structural change by DOPA incorporation pose the question of how their activity will be altered by Tyr hydroxylation. Redox-active PB-DOPA can generate radicals leading to enhanced oxidative damage, but has also been linked to peroxyl radical scavenging and antioxidant defense. The majority of bacterial DOPA-modified proteins identified to date are involved in carbohydrate metabolism (present study and ref. 27), which constitutes also a preferred target for BY-kinase–mediated Tyr phosphorylation and a prerequisite for virulence determinants such as capsule and biofilm formation.

Besides H_2O_2, the availability of intrabacterial iron, peroxidase activity (e.g., via compound I) and a low oxygen environment were required for p-Tyr conversion to DOPA. The intestinal niche is largely devoid of oxygen except for a 70-μm oxygenation zone

maintained by capillary diffusion (13). Oxygen measurements by electron paramagnetic resonance or phosphorescence oximetry detected luminal P_{O2} levels of 1–40 mmHg (≤5% O_2), depending on the section of the intestinal tract (32). Albeit lung P_{O2} levels are much higher, in pulmonary infection—and in particular in cystic fibrosis—anaerobic bacteria are frequently present, indicating a low oxygen environment. Propagation of bacteria in 21% oxygen does not reflect the in vivo situation for many mucosal pathogens. During oxidative stress modification of tyrosine residues to DOPA seems to occur frequently. PB-DOPA modifications were prominently associated with mitochondrial proteins in heart and brain tissues (33). The presence of H_2O_2 and transition metals in mitochondria creates an ideal environment for DOPA additions, and modified proteins included SOD2, cytochrome *c*, and ATPases (27, 33). Other DOPA-modified proteins were connected to oxidative stress pathways (NRF2, HSP90), the cytoskeletal regulatory network, or are multifunctional adapters (14-3-3 family) (33). Many of the modified Tyr residues in these proteins are predicted phosphorylation sites. Our study connects oxidative stress to interference with p-Tyr signaling by directly converting tyrosine residues that are associated with the catalytic activity of enzymes. Oxidative stress may likely trigger additional modifications throughout the protein, for example methionine oxidations. Tyrosine phosphorylation promotes not only signaling responses, but also affects protein localization and protein–protein interactions, and it is expected that many DOPA modifications caused by oxidative stress or mitochondrial dysfunction will disrupt protein networks, thereby altering numerous biological processes.

Materials and Methods

In vitro organ culture of human colon biopsies was performed as described previously (9). For infection studies and fetal lung explant studies, Sprague–Dawley rats and ligated rabbit ileal loops from Chinchilla rabbits were used. Ethical approval by the respective overseeing bodies was obtained. Fully informed consent was obtained from parents and, where appropriate, children. Ethical permission was obtained from the Ethics Committee of Our Lady's Childrens' Hospital Crumlin, Ireland. All animal procedures were performed after ethical approval from the Royal College of Surgeons in Ireland and licensed by the Department of Health and Children, Ireland or under the supervision of the Romanian National Sanitary Veterinary Agency (Law 471/2002, Government ordinance 37/2002) with approval of the Ethics Committee of Banat's University of Agricultural Sciences and Veterinary Medicine, King Michael I of Romania, Timisoara. Mass spectrometry, structural analysis, and graphical representations are described in *SI Materials and Methods*. Three-dimensional models of *K. pneumoniae* GAPDH-A (B5XS72_KLEP3) and *K. pneumoniae* AhpC (M7PUV9_KLEPN) were generated using the homology modeling program Modeler 9v14; molecular dynamics simulation and docking were performed with HADDOCK and evaluated in University of California, San Francisco Chimera. Detailed procedures and biochemical/microbiological methods are described in *SI Materials and Methods*.

ACKNOWLEDGMENTS. We thank N. Corcionivoschi for his contributions; K. O'Neill and C. King for technical assistance; C. Whitfield, P. Cossart, M. Baldus, C. Grangeasse, and J. Baugh for providing reagents; P. Nagy for discussions; and the staff and patients at the National Referral Center for Pediatric Gastroenterology, Our Lady's Children's Hospital Crumlin, Dublin, Ireland. The work was supported by the National Children Research Centre K/12/1 (to B.B. and U.G.K.); Science Foundation Ireland 10/IN.1/B2988 (to U.G.K.); and the COST Action BM1203 (to U.G.K. and L.A.A.).

1. Cameron EA, Sperandio V (2015) Frenemies: Signaling and nutritional integration in pathogen-microbiota-host interactions. *Cell Host Microbe* 18(3):275–284.
2. Kamada N, et al. (2012) Regulated virulence controls the ability of a pathogen to compete with the gut microbiota. *Science* 336(6086):1325–1329.
3. Imlay JA (2013) The molecular mechanisms and physiological consequences of oxidative stress: Lessons from a model bacterium. *Nat Rev Microbiol* 11(7):443–454.
4. Holmström KM, Finkel T (2014) Cellular mechanisms and physiological consequences of redox-dependent signalling. *Nat Rev Mol Cell Biol* 15(6):411–421.
5. Winterbourn CC, Kettle AJ (2013) Redox reactions and microbial killing in the neutrophil phagosome. *Antioxid Redox Signal* 18(6):642–660.
6. Wright CJ, et al. (2014) Characterization of a bacterial tyrosine kinase in *Porphyromonas gingivalis* involved in polymicrobial synergy. *MicrobiologyOpen* 3(3):383–394.
7. Chao JD, Wong D, Av-Gay Y (2014) Microbial protein-tyrosine kinases. *J Biol Chem* 289(14):9463–9472.
8. Corcionivoschi N, et al. (2012) Mucosal reactive oxygen species decrease virulence by disrupting *Campylobacter jejuni* phosphotyrosine signaling. *Cell Host Microbe* 12(1):47–59.
9. Lin MH, et al. (2009) Phosphoproteomics of *Klebsiella pneumoniae* NTUH-K2044 reveals a tight link between tyrosine phosphorylation and virulence. *Mol Cell Proteomics* 8(12):2613–2623.
10. Mancini S, Imlay JA (2015) The induction of two biosynthetic enzymes helps *Escherichia coli* sustain heme synthesis and activate catalase during hydrogen peroxide stress. *Mol Microbiol* 96(4):744–763.
11. Bilan DS, et al. (2013) HyPer-3: A genetically encoded $H_{(2)}O_{(2)}$ probe with improved performance for ratiometric and fluorescence lifetime imaging. *ACS Chem Biol* 8(3):535–542.
12. Hansen AM, et al. (2013) The *Escherichia coli* phosphotyrosine proteome relates to core pathways and virulence. *PLoS Pathog* 9(6):e1003403.
13. Marteyn B, Scorza FB, Sansonetti PJ, Tang C (2011) Breathing life into pathogens: The influence of oxygen on bacterial virulence and host responses in the gastrointestinal tract. *Cell Microbiol* 13(2):171–176.
14. Kröger C, et al. (2013) An infection-relevant transcriptomic compendium for *Salmonella enterica* Serovar Typhimurium. *Cell Host Microbe* 14(6):683–695.
15. Guengerich FP, Munro AW (2013) Unusual cytochrome p450 enzymes and reactions. *J Biol Chem* 288(24):17065–17073.
16. Alvarez LA, et al. (2013) Cj1411c encodes for a cytochrome P450 involved in *Campylobacter jejuni* 81-176 pathogenicity. *PLoS One* 8(9):e75534.
17. Prasad B, Mah DJ, Lewis AR, Plettner E (2013) Water oxidation by a cytochrome p450: Mechanism and function of the reaction. *PLoS One* 8(4):e61897.
18. Reuter M, van Vliet AH (2013) Signal balancing by the CetABC and CetZ chemoreceptors controls energy taxis in *Campylobacter jejuni*. *PLoS One* 8(1):e54390.
19. Shi L, et al. (2014) Evolution of bacterial protein-tyrosine kinases and their relaxed specificity toward substrates. *Genome Biol Evol* 6(4):800–817.
20. Lacour S, Bechet E, Cozzone AJ, Mijakovic I, Grangeasse C (2008) Tyrosine phosphorylation of the UDP-glucose dehydrogenase of *Escherichia coli* is at the crossroads of colanic acid synthesis and polymyxin resistance. *PLoS One* 3(8):e3053.
21. Chen YY, Ko TP, Lin CH, Chen WH, Wang AH (2011) Conformational change upon product binding to *Klebsiella pneumoniae* UDP-glucose dehydrogenase: A possible inhibition mechanism for the key enzyme in polymyxin resistance. *J Struct Biol* 175(3):300–310.
22. Houée-Lévin C, et al. (2015) Exploring oxidative modifications of tyrosine: An update on mechanisms of formation, advances in analysis and biological consequences. *Free Radic Res* 49(4):347–373.
23. Nagy P, Lechte TP, Das AB, Winterbourn CC (2012) Conjugation of glutathione to oxidized tyrosine residues in peptides and proteins. *J Biol Chem* 287(31):26068–26076.
24. Martyn KD, Frederick LM, von Loehneysen K, Dinauer MC, Knaus UG (2006) Functional analysis of Nox4 reveals unique characteristics compared to other NADPH oxidases. *Cell Signal* 18(1):69–82.
25. Mishra S, Imlay J (2012) Why do bacteria use so many enzymes to scavenge hydrogen peroxide? *Arch Biochem Biophys* 525(2):145–160.
26. Parsonage D, Karplus PA, Poole LB (2008) Substrate specificity and redox potential of AhpC, a bacterial peroxiredoxin. *Proc Natl Acad Sci USA* 105(24):8209–8214.
27. Lee S, et al. (2010) The first global screening of protein substrates bearing protein-bound 3,4-Dihydroxyphenylalanine in *Escherichia coli* and human mitochondria. *J Proteome Res* 9(11):5705–5714.
28. Pancholi V, Chhatwal GS (2003) Housekeeping enzymes as virulence factors for pathogens. *Int J Med Microbiol* 293(6):391–401.
29. Peralta D, et al. (2015) A proton relay enhances H2O2 sensitivity of GAPDH to facilitate metabolic adaptation. *Nat Chem Biol* 11(2):156–163.
30. Guo A, et al. (2008) Signaling networks assembled by oncogenic EGFR and c-Met. *Proc Natl Acad Sci USA* 105(2):692–697.
31. Bergt C, Fu X, Huq NP, Kao J, Heinecke JW (2004) Lysine residues direct the chlorination of tyrosines in YXXK motifs of apolipoprotein A-I when hypochlorous acid oxidizes high density lipoprotein. *J Biol Chem* 279(9):7856–7866.
32. Albenberg L, et al. (2014) Correlation between intraluminal oxygen gradient and radial partitioning of intestinal microbiota. *Gastroenterology* 147(5):1055–1063.e8.
33. Zhang X, et al. (2010) Endogenous 3,4-dihydroxyphenylalanine and dopaquinone modifications on protein tyrosine: Links to mitochondrially derived oxidative stress via hydroxyl radical. *Mol Cell Proteomics* 9(6):1199–1208.
34. Renault M, et al. (2012) Cellular solid-state nuclear magnetic resonance spectroscopy. *Proc Natl Acad Sci USA* 109(13):4863–4868.
35. Turriziani B, et al. (2014) On-beads digestion in conjunction with data-dependent mass spectrometry: A shortcut to quantitative and dynamic interaction proteomics. *Biology (Basel)* 3(2):320–332.
36. Phillips JC, et al. (2005) Scalable molecular dynamics with NAMD. *J Comput Chem* 26(16):1781–1802.
37. de Vries SJ, van Dijk M, Bonvin AM (2010) The HADDOCK web server for data-driven biomolecular docking. *Nat Protoc* 5(5):883–897.
38. van Dijk AD, Bonvin AM (2006) Solvated docking: Introducing water into the modelling of biomolecular complexes. *Bioinformatics* 22(19):2340–2347.
39. Oh E, Jeon B (2014) Role of alkyl hydroperoxide reductase (AhpC) in the biofilm formation of *Campylobacter jejuni*. *PLoS One* 9(1):e87312.